**Peter KOSMATIN, Damijan MILJAVEC, Danjel VONČINA**

University of Ljubljana, Faculty of Electrical Engineering

# A novel control strategy for the switched reluctance generator

***Abstract***. *The paper proposes a novel switching strategy that increases the efficiency of the energy conversion and reduces the noise level produced by the generator. The technique redistributes the three switching stages of the converter within one working cycle. Such technique is viable when the generator operates below its base speed. Here, the back electromagnetic force is always lower than the DC-link voltage, hence the phase current is controlled at a desired value. The proposed control method is validated using a commercially available four phase 8/6 switched reluctance generator.*

***Streszczenie.*** *W artykule zaproponowano nową strategię przełączania generator reluktancyjnego. Metoda zwiększa skuteczność konwersji energii I redukuje szumy. W jednym cyklu realizuje się trzy etapy przełączeń. Metoda jest zalecana gdy generator operuje poniżej bazowej szybkości. (**Nowa strategia sterowania generatorem reluktancyjnym**)*

**Keywords:** acoustic noise, asymmetric bridge converter, current control, efficiency, switched reluctance generator.
**Słowa kluczowe:** generator reluktancyjny, przełączanie, szumy

## Introduction

To enable energy conversion, the switched reluctance (SR) machine utilizes variable inductance enabled by laminated salient poles on its stator and rotor. As rotor carries no windings or permanent magnets its size is small with low inertia. The stator poles are equipped with concentrically wound phase windings, thus simplifying the manufacture. As there is no winding distribution between the different stator slots, each winding is electrically independent for which reason the mutual coupling between phases is negligible. Consequently, an electrical fault in one of the phases does in general not affect the other phases. Because of the sequential energizing of the stator phases, there is a need for the SR machine to use a controllable converter for its operation. Hence, the SR machines are used in variable-speed drive systems and because of their simple construction in applications demanding either high-speed or/and high-temperature operation [1]. On the other hand, the sequential energizing of the stator phases is the reason for several disadvantages. Such operation of the SR machines produces torque ripple and gives rise to the acoustic noise and vibrations.

By adjusting the converter switching angles, the SR machine can operate either as a motor or as a generator [2]. In recent years, the SR generator has gained more attention from researchers for its applicability in wind-energy conversion systems, aerospace power systems, starter/generator applications in hybrid vehicles and even in small experimental DC-grid power systems [3-6]. In the SR generator drives, the value of the back-EMF defines the control strategy that can be used to control either the output electric power or the DC-link voltage. At a higher rotational speed the back-EMF is higher than the DC-link voltage and the phase current is controlled exclusively by the turn-on ($\theta_{on}$) and the turn-off angle ($\theta_{off}$). Here, the SR generator enters the single-pulse mode. In low-speed operation with the back-EMF lower than the DC-link voltage, the phase current is kept at the desired value by using the pulse-width modulation (PWM) or the hysteresis control technique.

The converter most commonly used in driving the SR generator is the asymmetric bridge converter providing three switching possibilities for controlling the phase currents. The previously published research is focused on the use of adaptive control schemes to compensate for the SR generator non-linear magnetic characteristics. The authors also proposed switching-angles control algorithms to optimize the efficiency regardless of the SR generator working point [7-9].

The focus of the paper is on maximizing efficiency of the energy conversion when using an asymmetric bridge converter as a drive unit for the SR generator. The presented current-control technique incorporates the converter interchangeable switching stages when the SR generator operates below its base speed. The influence of the proposed current-control technique on the efficiency and also on the emitted noise levels produced by the SR generator is experimentally verified.

## Analysis of the SR generator drive efficiency

When the stator phases are energized sequentially, the mutual coupling between them can be neglected. The voltage equation for the equivalent electric circuit is given by

$$u_{ph} = R_{ph} i_{ph} + \frac{d\psi\left(i_{ph}, \theta\right)}{dt}. \tag{1}$$

Here, applied voltage $u_{ph}$ is equal to the sum of the resistive-voltage drop and the rate of the flux-linkage $\psi(i_{ph}, \theta)$ change, which is a function of phase current $i_{ph}$ and rotor position $\theta$, because of the magnetic nonlinearity of the ferromagnetic material and salient stator and rotor poles. If magnetic saturation is ignored, the equation takes the below simplified form:

$$u_{ph} = R_{ph} i_{ph} + L\left(\theta\right)\frac{di_{ph}}{dt} + i_{ph}\omega\frac{dL\left(\theta\right)}{d\theta}. \tag{2}$$

In (2) the flux-linkage is replaced by the product of phase inductance $L(\theta)$ and phase current $i_{ph}$. The three terms on its right side are the resistive-voltage drop, inductive-voltage drop and back-EMF $e_g$.

The phase current usually being unipolar when using most of the power converters suitable for driving the SR generator, the sign of the back-EMF, and therefore also the region in which the generator operates, is determined by the slope of the phase inductance. If the stator phases are energized during the negative slope of the inductance, the back-EMF opposes the applied voltage and the SR machine operates in the generating region. With the rotor pole moving away from the position aligned with the stator pole, the negative torque is produced and the mechanical energy is extracted from the prime mover and converted to the electrical. The equation for electromagnetic torque $T_e$ can be obtained from the (2) under assumption that the sum of the converted electric and magnetic energy equals the mechanical energy.

(3) $$T_e\left(i_{ph},\theta\right)=\frac{1}{2}i_{ph}^2\frac{dL\left(\theta\right)}{d\theta}$$

Because of the non-sinusoidal flux waveform, the SR generator drive losses are calculated by using the off-line 2D or 3D finite-element method [10] or they can be roughly estimated using the below equations for iron $P_{fe}$ and copper losses $P_{cu}$.

(4) $$P_{fe}=c_h fB^{a+bB}+c_e\left(\frac{dB}{dt}\right)^2$$

(5) $$P_{cu}=qI_{ph,rms}^2R_{ph}$$

Here, the symbol $R_{ph}$ represents the phase resistance. Hysteresis $c_h$ and eddy-current $c_e$ loss coefficients along with coefficients $a$ and $b$ can be obtained from the loss curves given by the manufacturer. Frequency $f$ is defined by the product of the number of phases $q$ and frequency of the phase current $f_c$.

(6) $$f=qf_c$$

For on-line validation of different control strategies to be accurate, input mechanical $P_{meh}$ and output electric power $P_{el}$ have to be measured, thus determining the efficiency $\eta$.

(7) $$\eta=\frac{P_{el}}{P_{meh}}$$

**Analysis of the noise and vibration generation sources**

In electric machines there are four main sources generating the noise: aerodynamic, electronic, magnetic and mechanical [1]. The aerodynamic noise is induced by the salient construction of the rotating rotor and is enhanced by the fan-based cooling mechanism mounted on the rotor. In the electronic source category, the noise is emitted by the harmonics applied in the voltage and phase currents. It is known that pulse-width modulation when controlling the phase current, produces a lower noise than the hysteresis current controller. Also, it is recommended to use the highest possible switching frequency to minimize the current ripple. Besides the load-induced mechanical noise (couplings, foundation), the noise induced by bearings and rotor eccentricity, the stator vibration is the main source generating the mechanical and also the SR machine noise. The stator vibrations are caused by radial forces produced by the magnetic flux passing across the air gap. When the magnetic flux passes across the air gap in the radial direction from the stator pole to the rotor, three kinds of forces are induced: tangential $F_t$, radial $F_r$ and lateral $F_l$. The tangential force produces the electromagnetic torque of the SR machine, while the radial and lateral forces affect its structure. To analytically evaluate the magnitude of these forces without using the computer-aided 2D or 3D finite-element method [11], some simplifications to the mathematical model of the SR machine have been made by other authors [1]. In these simplifications, iron of the stator and rotor cores is infinitely permeable, i.e. the reluctance is zero. So, only the air gap provides reluctance in an equivalent magnetic circuit from which the following equations are derived [1]:

(8) $$F_t=\frac{l_g L}{2\mu_0}B_g^2\left(\theta,l_g,i\right),$$

(9) $$F_r=-\frac{r_r L\theta}{2\mu_0}B_g^2\left(\theta,l_g,i\right),$$

(10) $$F_l=\frac{l_g r_r\theta}{2\mu_0}B_g^2\left(\theta,l_g,i\right),$$

where: $l_g$ – length of an air gap, $r_r$ – outer radius of the rotor, $L$ – stack length of the machine, $\theta$ – stator and rotor pole overlap angle, $\mu_0$ – vacuum permeability, $B_g$ – air gap flux density.

As seen from (9), radial force $F_r$ is the largest when the stator and rotor poles are aligned. It is also the largest compared to tangential force $F_t$ and lateral force $F_l$.

(11) $$\frac{F_r}{F_t}=-\frac{r_r\theta}{l_g}$$

While the tangential and lateral forces are of a similar magnitude, the ratio between radial force $F_r$ and tangential force $F_t$ indicates that the radial force is always a multiple of the tangential force. With a non-uniform air gap such large force affects the yoke and salient poles of the machines. The rotor is less affected because of its rigidness [12], while the stator tends to vibrate, thus producing the main noise source in the SR machines [13].

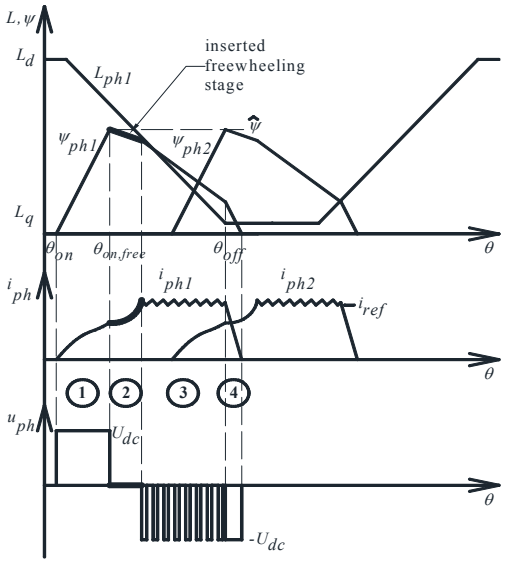


Fig. 1. Ideal phase inductance $L$, flux-linkage $\psi$, phase current $i_{ph}$ and phase voltage $u_{ph}$ waveforms for an SR generator operating at a low speed with the proposed control strategy.

The magnitude of the stator vibrations because of which the stator tends to take on an oval shape is also affected by the frequency of phase current $f_c$ and natural vibration frequency of the stator [14,15]. If the natural vibration frequency is an odd harmonic of the phase current frequency, the resonance occurs and the magnitude of the stator vibrations increases. On the contrary, with an even harmonic of the phase current frequency the vibrations are significantly reduced. Frequency $f_c$ is defined by the number of rotor poles $N_r$ and angular speed $\omega$

(12) $$f_c=\frac{\omega}{2\pi}N_r.$$

As known the change in the stator phase voltage generates stator vibrations and larger vibrations are produced when the voltage change takes place near the

aligned position. To limit these vibrations, authors propose some basic construction guidelines [2] or apply different switching strategies. These strategies are mostly used for a particular type of the converter such as two-stage or three-stage commutation method [16] or are recommended in general such as the random-frequency PWM switching strategy [17]. All these strategies avoid using the hard-switching control method where the value of the changed phase voltage is twice the value of the supply voltage.

**The proposed switching strategy**

When using the asymmetric bridge converter to control the SR generator, there are three switching stages that can be interchanged in order to maximize the efficiency of the drive. These are the magnetizing, demagnetizing and freewheeling switching stage. During the magnetizing stage (Fig. 1. – Section 1) in which both transistors in the phase leg are turned on, the stator phase is affected by the full DC-link voltage, thus making the phase current to rise. Because of the low-speed operation, the back-EMF is always lower than the semi-constant DC-link voltage. When the phase current reaches its reference value $i_{ref}$, the magnetizing switching stage is replaced by either the demagnetizing or the freewheeling stage so as to maintain the phase current within a small hysteresis $\Delta i_{ph}$ (Fig. 1. – Section 3). The start and end of the working cycle are marked with turn-on $\theta_{on}$ and turn-off $\theta_{off}$ angle, respectively. At turn-off angle $\theta_{off}$, both transistors in the phase leg are turned off and the current gradually falls to zero (Fig. 1. – Section 4). The above described switching strategy is named the standard switching strategy and its details can be found in literature [2, 7, 8].

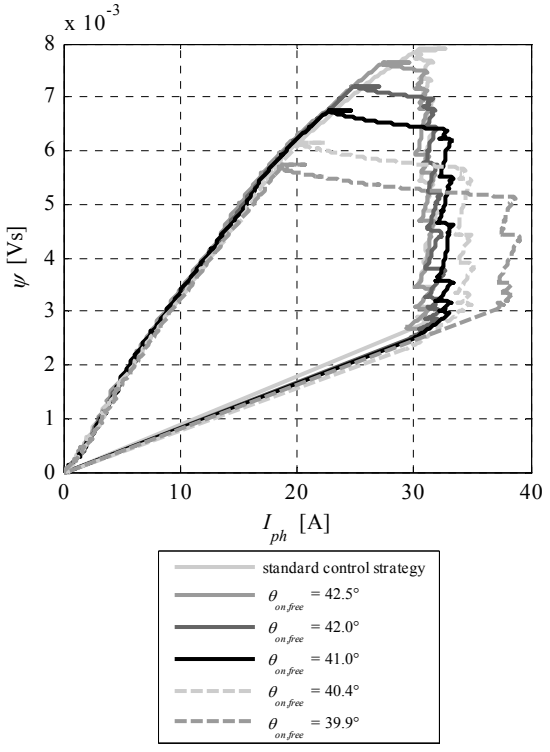


Fig. 2. Flux-linkage curves varying the $\theta_{on,free}$ angle at 3000 rpm, 30 V DC-link voltage and at 150 W load power. The turn-on and turn-off angle are set at 33° and 51°, respectively.

By changing the sequence order of the three switching stages (magnetizing, demagnetizing, freewheeling), the proposed switching strategy increases the efficiency of the SR generator drive and decreases vibrations induced by the voltage change of the stator phase. The proposed modification assumes that by decreasing the maximum value of phase flux-linkage $\psi(i_{ph}, \theta)$, the value of magnetic field $B$ and therefore also iron losses $P_{fe}$ (4) and radial force $F_r$ (9) decrease correspondingly.

$$\psi = Li_{ph} = N\int_A \bar{B}d\bar{A} \tag{13}$$

As seen in (13), the flux-linkage is proportional to the product value of phase inductance $L$ and current $i_{ph}$. It is therefore important to minimize this product to decrease the iron losses and the induced acoustic noise. Product $L \cdot i_{ph}$ is minimized by inserting the freewheeling switching stage (Fig. 1. – Section 2) before the phase current reaches its reference value. The start of the freewheeling stage is marked with angle $\theta_{on,free}$, during which the phase winding is short-circuited and the phase current tends to rise with the back-EMF as the only voltage source. The current rise time is prolonged and the maximum value of product $L \cdot i_{ph}$ is therefore lowered (Fig. 2.). Also, during the freewheeling stage, no energy is extracted from the DC-link.

Table 1. Specifications of the SR generator

| *Parameter* | *Value* |
|---|---|
| Output power | 1.2 kW |
| Rated speed | 3000 rpm |
| Rated voltage | 30 V |
| Rated current | 65 A |
| Number of phases $q$ | 4 |
| Phase resistance $R_{ph}$ | 40 mΩ |
| Number of stator poles $N_s$ | 8 |
| Number of rotor poles $N_r$ | 6 |
| Unsaturated unaligned inductance $L_u$ | 115 μH |
| Unsaturated aligned inductance $L_a$ | 645 μH |

**Experimental validation of the proposed switching strategy**

The proposed switching strategy was validated by using a commercially available four phase SR generator with eight stator and six rotor poles. Its properties are listed in Table 1. The converter topology was an asymmetric bridge converter with the MOSFET-type transistors. Also to be mentioned is that the measurements were conducted at a fixed turn-on $\theta_{on}$ (33°) and turn-off $\theta_{off}$ (51°) angle optimized for the following working point: 30 V of the DC-link voltage, 3000 rpm and 150 W of the load power.

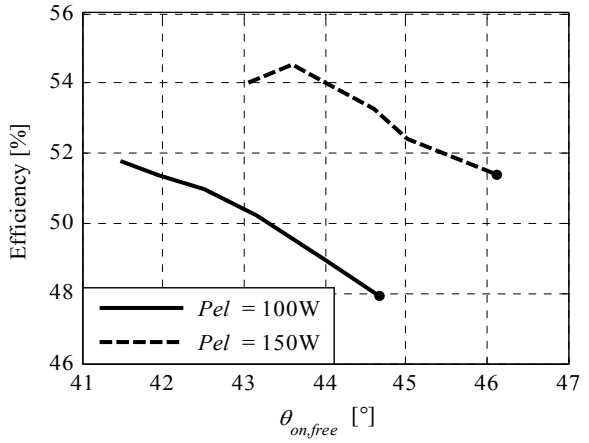


Fig. 3. Efficiency when varying the $\theta_{on,free}$ angle at 2500 rpm, 20 V DC-link voltage and variable load power. The turn-on and turn-off angle are set at 33° and 51°, respectively. The efficiency value marked with a dot corresponds to the standard control strategy.

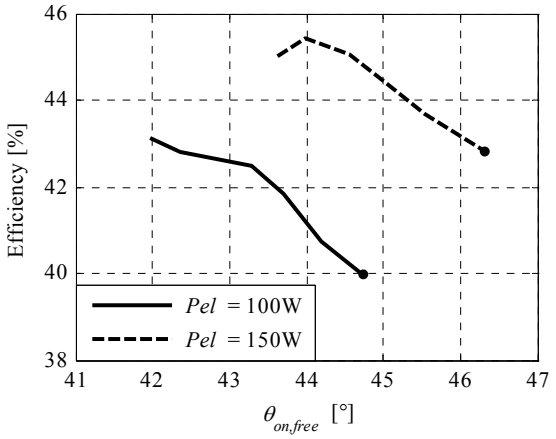


Fig. 4. Efficiency when varying the $\theta_{on,free}$ angle at 3000 rpm, 20 V DC-link voltage and variable load power. The turn-on and turn-off angle are set at 33° and 51°, respectively. The efficiency value marked with a dot corresponds to the standard control strategy.

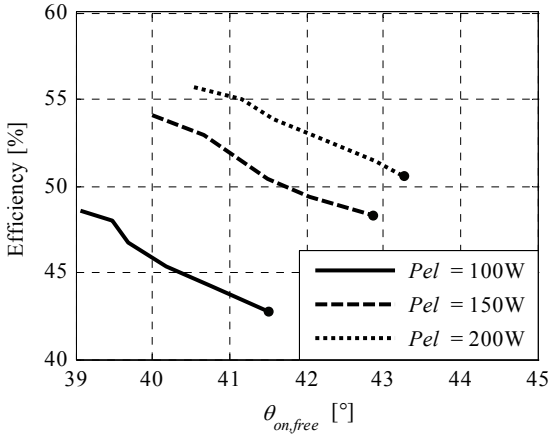


Fig. 5. Efficiency when varying the $\theta_{on,free}$ angle at 2500 rpm, 30 V DC-link voltage and variable load power. The turn-on and turn-off angle are set at 33° and 51°, respectively. The efficiency value marked with a dot corresponds to the standard control strategy.

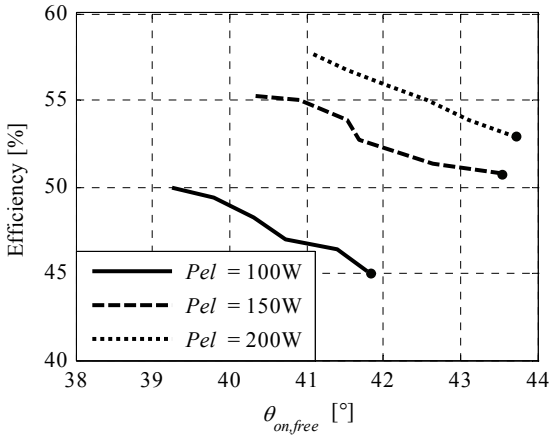


Fig. 6. Efficiency when varying the $\theta_{on,free}$ angle at 3000 rpm, 30 V DC-link voltage and variable load power. The turn-on and turn-off angle are set at 33° and 51°, respectively. The efficiency value marked with dots corresponds to the standard control strategy.

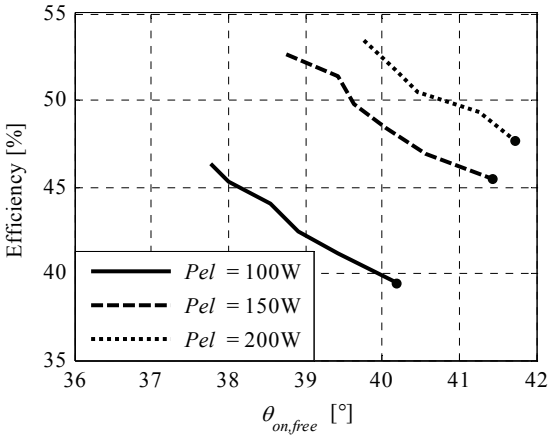


Fig. 7. Efficiency when varying the $\theta_{on,free}$ angle at 2500 rpm, 40 V DC-link voltage and variable load power. The turn-on and turn-off angle are set at 33° and 51°, respectively. The efficiency value marked with a dot corresponds to the standard control strategy.

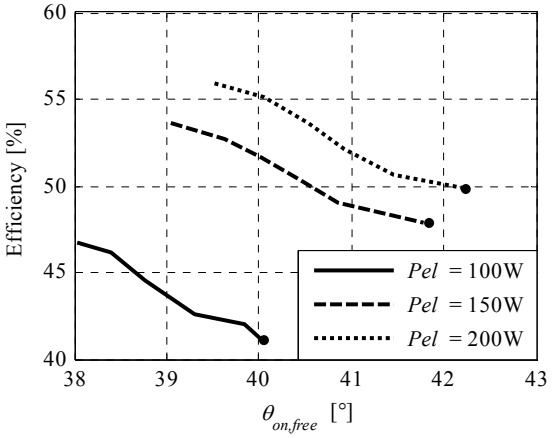


Fig. 8. Efficiency when varying the $\theta_{on,free}$ angle at 3000 rpm, 40 V DC-link voltage and variable load power. The turn-on and turn-off angle are set at 33° and 51°, respectively. The efficiency value marked with a dot corresponds to the standard control strategy.

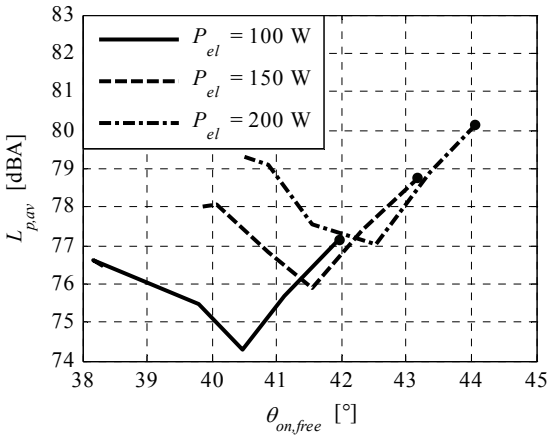


Fig. 9. A-weighted sound pressure level of the SR generator drive when varying the $\theta_{on,free}$ angle at 3000 rpm, 30 V DC-link voltage and variable load power $P_{el}$. The turn-on and turn-off angle are set at 33° and 51°, respectively. The sound pressure level marked with dots corresponds to the standard control strategy.

*Measurement of the SR generator drive efficiency*

Besides decreasing the noise level of the SR generator drive, the proposed switching strategy also increases its efficiency. To demonstrate the latter, a series of measurements was conducted at various working points. Here, DC-link voltage $U_{dc}$, rotational speed $\omega$ and load power $P_{el}$ varied while the turn-on $\theta_{on}$ and turn-off angle $\theta_{off}$ were fixed. The increase in the efficiency is shown by varying angle $\theta_{on,free}$ introduced with the proposed switching strategy (Figs. 3 – 8). The figures confirm the theoretically assumed considerable increase in the efficiency compared to the standard control strategy.

*Acoustic-noise measurement*

The noise level was measured in a large room with eight sample positions distributed around the test subject at the distance of one meter. The measurement was conducted using a sound pressure meter. The background noise during the measurement was constant at 55 dBA. The measurements were then averaged using the following equation

$$L_{p,av} = 10\log\left(\frac{1}{N}\sum_{i=1}^{N} 10^{\frac{L_{p,i}}{10}}\right), \tag{14}$$

where: $L_{p,i}$ – A-weighted sound pressure level at a sample position, $L_{p,av}$ – A-weighted average sound pressure level over all sample positions, $N$ – number of the sound level meter positions.

It should be noted that by measuring the sound pressure level there was no tendency to determine the absolute value of the noise level produced by the SR generator drive, but to evaluate the difference in the sound pressure levels when applying the proposed switching strategy.

In Fig. 9. there is a considerable decrease noticed in the sound pressure level when applying the freewheeling switching stage after the initial magnetization stage.

The reason for the noticeable local minimum is the dependence of the stator vibration to the time between two major changes in phase voltage. If the time length of the inserted freewheeling switching stage is close to the half of the stator vibration resonant period, the vibration is limited similarly to the extended zero-voltage loop method [1,16].

By increasing the SR generator load with the consequential increase in the maximum value of the phase current, the sound pressure level also rises, as seen in Fig. 9.

**Conclusion**

The paper proposes a novel switching strategy for the SR generator operating at a low rotational speed with the back-EMF always lower than the controlled DC-link voltage. The strategy introduces a new switching angle $\theta_{on,free}$ in the current-control algorithm in order to increase the efficiency of the generator. By using the proposed strategy the conversion efficiency at the measured working points is increased by roughly 5% while the noise level emitted by the SR generator drive is decreased by approximately 3 dBA. The strategy can be used for the asymmetric bridge converter as a drive unit for the SR generator.

REFERENCES


[1] Krishnan R., Switched reluctance motor drives: modeling, simulation, analysis, design and applications, *Industrial electronics series*, 2001.

[2] Miller T. J., Electronic control of switched reluctance machines, *Newnes power engineering series, Reed educational and professional publishing*, 2001.

[3] Cardenas R., Pena R., Perez M. and Clare J., Control of a switched reluctance generator for variable-speed wind energy applications, *IEEE transactions on energy conversion*, vol. 20, no. 4, Dec. 2005.

[4] Powell D. J., Jewell G. W., Calverley S. D. and Howe D., Iron loss in a modular rotor switched reluctance machine for the "More-Electric" aero-engine, *IEEE transactions on magnetics*, vol. 41, no. 10, pp. 3934- 3936, Oct. 2005.

[5] Schofield N. and Long S., Generator operation of a switched reluctance starter/generator at extended speeds, *IEEE transactions on vehicular technology*, vol. 58, no. 1, pp. 48-56, Jan. 2009.

[6] Chang Y. C. and Liaw C. M., Establishment of a switched-reluctance generator-based common DC microgrid system, *IEEE transactions on power electronics*, vol. 26, no. 9, pp. 2512-2527, Sept. 2011.

[7] Mademlis C. and Kioskeridis I., Optimizing performance in current-controlled switched reluctance generators, *IEEE transactions on energy conversion*, vol. 20, no. 3, pp. 556-565, Sept. 2005.

[8] Torrey D. A., Switched reluctance generators and their control, *IEEE transactions on industrial electronics*, vol. 49, no. 1, Feb. 2002.

[9] Chang Y. C. and Liaw C. M., On the design of power circuit and control scheme for switched reluctance generator, *IEEE transactions on power electronics*, vol. 23, no. 1, Jan. 2008.

[10] Prus V., Nikitina A., Zagirnyak M., Miljavec D., Research of energy processes in circuits containing iron in saturation condition, Przegląd Elektrotechniczny, no. 3, pp. 149-152, 2011.

[11] Leskovec J., Makuc D., Lahajnar F., Miljavec D., Nonlinear reluctance model of transverse flux motor, *Przegląd Elektrotechniczny*, no. 3, pp. 111-114, 2011.

[12] Ellison A. J., Mech F. I. and Moore C. J., Acoustic noise and vibration of rotating electric machines, *IEE proceedings*, vol. 115, no. 1, pp. 1633-1640, Nov. 1968.

[13] Wu C. Y. and Pollock C., Analysis and reduction of vibration and acoustic noise in the switched reluctance drive, *IEEE transactions on industry applications*, vol. 31, no. 1, pp. 91-98, Jan./Feb. 1995.

[14] Fiedler J. O., Kasper K. A. and De Doncker R. W., Calculation of the acoustic noise spectrum of SRM using modal superposition, *IEEE transactions on industrial electronics*, vol. 57, no. 9, pp. 2939-2945, Sept. 2010.

[15] Anwar M. N., Radial force calculation and acoustic noise prediction in switched reluctance machines, *IEEE transactions on industry applications*, vol. 36, no. 6, pp. 1589-1597, Nov./Dec. 2000.

[16] Pollock C. and Wu C. Y., Acoustic noise cancellation techniques for switched reluctance drives, *IEEE transactions on industry applications*, vol. 33, no. 2, pp. 477-484, March/April 1997.

[17] Chai J.Y., Lin Y. W. and Liaw C. M., Comparative study of switching controls in vibration and acoustic noise reductions for switched reluctance motor, *IEEE transactions on power applications*, vol. 153, no. 3, pp. 348-360, May 2006.



***Authors**: B.Sc. Peter Kosmatin, E-mail: peter.kosmatin@fe.uni-lj.si; prof. Ph.D. Damijan Miljavec, E-mail: damijan.miljavec@fe.uni-lj.si; prof. Ph.D. Danjel Vončina, E-mail: voncina@fe.uni-lj.si; All the authors are with University of Ljubljana, Faculty of Electrical Engineering, Department of Mechatronics, Trzaska cesta 25, 1000 Ljubljana, Slovenia.*